Available online at www.sciencedirect.com
SCIENCE DIRECT
International Journal of Heat and Mass Transfer 49 (2006) 3681–3690
International Journal of HEAT and MASS TRANSFER
www.elsevier.com/locate/ijhmt

On temperature prediction at low Re turbulent flows using the Churchill turbulent heat flux correlation

Phuong M. Le [a], Dimitrios V. Papavassiliou [a,b,*]

[a] School of Chemical, Biological and Materials Engineering, The University of Oklahoma, 100 East Boyd St., SEC T-335, Norman, OK 73019, USA
[b] Sarkeys Energy Center, The University of Oklahoma, 100 East Boyd St., SEC T-335, Norman, OK 73019, USA

Received 4 November 2005; received in revised form 9 February 2006
Available online 17 April 2006

Abstract

The present work investigates the prediction of mean temperature profiles in turbulent channel flow using the fraction of the heat flux due to turbulence. According to this new model, suggested by Churchill and co-workers, fully developed flow and convection can be expressed as local fractions of the shear stress and the heat flux density due to turbulent fluctuations, respectively. The fully developed temperature profile can be predicted if the velocity field and the turbulent Prandtl number are known. Temperature profiles for Pr between 0.01 and 50,000 have been obtained theoretically and with simulations through the use of Lagrangian methods for both plane Poiseuille flow and plane Couette flow. The half channel height for all simulations was $h = 150$ in wall units. The theoretical predictions have been found to agree with the data quite well for a range of Pr, but there are deviations at very high Pr.

Keywords: Prandtl number; Turbulent transport; Lagrangian methods; Algebraic models

1. Introduction

Scaling questions about the law of the wall (a bulwark of turbulence theory) in low and intermediate Reynolds numbers (i.e., flow in channels and pipes, instead of infinite boundary layers) have been raised for the velocity field [1–7]. It is now argued that turbulence quantities do not scale with the viscous wall parameters, as defined conventionally, and that a Reynolds number effect is present. Similar issues can be raised for the equivalent of the law of the wall for heat transfer. Results from direct numerical simulations have shown that scaling with the wall parameters for low Reynolds numbers does not provide universal behavior for the fluctuating thermal field [8–10]. However, an effort to explore the scaling of heat transfer similar to that for momentum has not been vigorously pursued, with the notable exception of Churchill and coworkers [11–14] who suggested the use of the local fraction of the heat flux density due to turbulent fluctuations to predict the mean temperature, introducing, thus, the use of a scale different than the conventional friction temperature.

An algebraic model for the prediction of mean turbulence quantities was first introduced by Churchill and Chan [11] in 1995; it has been suggested to be superior in several aspects when compared with other conventional algebraic models that are based on empiricisms and approximations. Heuristic concepts, like the eddy diffusivity or the mixing length that are not fundamentally sound, are totally avoided. According to this new model, fully developed flow and convection can be expressed as fractions, respectively, of shear stress and heat flux density due to turbulent fluctuations. The mean temperature profile can be predicted based on exact equations, given the velocity profile and the turbulent Prandtl number. This is a very significant

* Corresponding author. Address: School of Chemical, Biological and Materials Engineering, The University of Oklahoma, 100 East Boyd St., SEC T-335, Norman, OK 73019, USA. Tel.: +1 405 3255811; fax: +1 405 3255813.
E-mail address: dvpapava@ou.edu (D.V. Papavassiliou).

0017-9310/$ - see front matter © 2006 Elsevier Ltd. All rights reserved.
doi:10.1016/j.ijheatmasstransfer.2006.02.022

Nomenclature

C_f	correction factor defined in Eqs. ((22))
C_p	specific heat at constant pressure (kJ/(kg K))
E_α	eddy diffusivity (kg/(m s))
E_v	eddy viscosity (kg/(m s))
h	half height of the channel (m)
k	thermal conductivity (W/(m K))
P_1	conditional probability for a marker to be at a location (x,y) at time t, given that it was released at a known time from a known location at the channel wall
P_2	joint probability for a marker to be at a location (x,y)
Pr	Prandtl number, $Pr = v/\alpha$
Pr_t	turbulent Prandtl number, $Pr_t = E_v/E_\alpha$
q	heat flux (kW/m^2)
Re	Reynolds number, $Re = U_c h/v$
T	temperature (K)
T^*	friction temperature, $T^* = q_w/(\rho C_p u^*)$
$\overline{T}$	mean temperature (K)
T'	temperature fluctuation (K)
$\overline{T'v'}$	normal heat flux
t	time (s)
t_0, t_f	initial and final time of tracking markers (s)
U	velocity (m/s)
$\overline{U}$	mean velocity (m/s)
$u*$	friction velocity, $u^* = (\tau_w/\rho)^{1/2}$ (m/s)
$\overline{u'v'}$	normal shear stress
x, y, z	streamwise, normal and spanwise coordinates
X, Y	Lagrangian displacement of a marker from the source in the x, y directions

Greek symbols

α	thermal diffusivity (m^2/s)
γ	correction term defined in Eq. (6)
v	kinematic viscosity (m^2/s)
π	trigonometric pi ($\pi = 3.14159\ldots$)
ρ	fluid density (kg/m^3)
σ	standard deviation of the pdf that describes the diffusive motion of the heat markers
τ	shear stress (Pa)

Superscripts and subscripts

$\overline{()}$	ensemble average
$\vec{()}$	vector quantity
$()^+$	value made dimensionless with the wall parameters
$()^{++}$	local fraction due to turbulence
$()^*$	friction value
$()_0$	value at the instant of marker release
$()_w$	value at the wall of the channel

contribution in the area of turbulent convection, especially given the semi-empirical predictive capabilities of the past [15]. In addition, the concept of a scale that is directly associated with turbulence, like the fraction of the local heat flux due to turbulence suggested by Churchill, seems more natural, when contrasted to scaling based on the wall friction temperature (which is dependent only on viscous effects). In other words, since the temperature fluctuations are generated due to velocity fluctuations and their production occurs within the conductive wall layer but not at the wall, it makes sense to predict turbulent transfer based on a turbulence quantity rather than a viscous one.

Churchill et al. [16] have recently conducted an analysis of the sensitivity of the new algebraic model to the numerical empiricisms and empirical functions that enter into it. They found that predictions are rather insensitive to reasonable changes in the empirical parameters of the model. On the other hand, comparison of the model predictions to either simulation results or experimental measurements for a truly extensive range of data has not been reported. This is the space that the present paper covers: the verification of the Churchill model for a range of fluids (i.e., a range of Prandtl numbers) and for fundamentally different turbulent velocity fields (i.e., pressure driven and shear driven). Our research group has used direct numerical simulation (DNS) in conjunction with Lagrangian scalar tracking (LST) to study turbulent transport for an extensive range of Prandtl numbers (from $Pr = 0.01$ to 50,000) in Poiseuille channel flow [17,18] and in Couette flow [18,19]. Mean temperature profile predictions through this method agree very well with previous experimental and direct numerical simulation results, and, quite importantly, they have been obtained with a consistent methodology that has been used for a range of cases where conventional Eulerian direct simulations are not yet feasible.

2. Background and theory

2.1. Eulerian heat transfer

In the Eulerian framework, the temperature T can be decomposed into the mean temperature $\overline{T}$ and the fluctuation T'. The temperature is conventionally made dimensionless by normalizing with the friction temperature T^*, $T^* = q_w/(\rho C_p u^*)$, where q_w is the heat flux at the wall defined in terms of the thermal conductivity of the fluid k as

$$q_w = -k\left(\frac{d\overline{T}}{dy}\right)_w \tag{1}$$

Therefore, a dimensionless temperature T^+ can be calculated by

$$T^+ = \frac{T}{T^*} = -\frac{T\rho C_p u^*}{k\left(\frac{d\overline{T}}{dy}\right)_w} = -Pr\frac{T}{\left(\frac{d\overline{T}}{dy^+}\right)_w} \tag{2}$$

2.2. The Churchill algebraic model

We present here a brief overview of the model – more details can be found in the original publications. Churchill and Chan [11] have rewritten the time-averaged, once-integrated differential representation for the conservation of momentum for fully developed turbulent flow field as

$$\frac{\tau}{\tau_w} = \frac{d\overline{U}^+}{dy^+} + \overline{(u'v')}^+ \tag{3}$$

where y^+ is the distance from the wall in viscous wall units and ($y^+ = yu^*/\nu$), $\overline{U}^+$ is the dimensionless mean velocity ($\overline{U}^+ = \overline{U}/u^*$). They have also derived and introduced the dimensionless quantity $\overline{(u'v')}^{++}$, which represents the local fraction of the shear stress due to fluctuations in velocity. Eq. (3) therefore was written as

$$\frac{\tau}{\tau_w}\left[1 - \overline{(u'v')}^{++}\right] = \frac{d\overline{U}^+}{dy^+} \tag{4}$$

where $\overline{(u'v')}^{++} = -\rho\overline{u'v'}/\tau$.

In analogy to momentum transfer, turbulent heat transfer based on the fraction of the heat flux that is due to turbulence has been studied more deeply in recent papers by Churchill and coauthors [12,14,20,21]. These papers were focused on the temperature predictions in turbulent flow fields, in round tubes [20] and between parallel plates [21]. The time-averaged energy balance for steady, fully developed convection in the turbulent flow of a Newtonian fluid between parallel plates was rewritten in terms that utilized the local fraction of the heat flux due to fluctuations $\overline{T'v'}^{++}$

$$\frac{q}{q_w}\left[1 - \overline{(T'v')}^{++}\right] = \frac{dT^+}{dy^+} \tag{5}$$

where $\overline{(T'v')}^{++} = -\rho C_p\overline{T'v'}/q$.

In Refs. [11,12,14,20,21], Churchill and coauthors have also discussed an effect that has been neglected in previous research: the deviation of the heat flux density distribution due to the shear stress distribution across the channel. They have suggested the use of the correction term γ, which can be included in the calculation of the heat flux ratio, as shown in the following equations for equal and uniform heating from one plate, Eq. (6a) and two plates, Eq. (6b), respectively:

$$\frac{q}{q_w} = (1+\gamma)\left(1 - \frac{y^+}{2h^+}\right) \tag{6a}$$

$$\frac{q}{q_w} = (1+\gamma)\left(1 - \frac{y^+}{h^+}\right) \tag{6b}$$

From Eqs. (4), (5) and (6b), temperature profiles can be calculated by integration for the case where two plates are heated uniformly and equally [21]

$$\overline{T}^+ = Pr\int_0^{y^+} \frac{(1+\gamma)\left(1-\frac{y^+}{h^+}\right)}{1 + \frac{Pr}{Pr_t}\left(\frac{\overline{(u'v')}^{++}}{1-\overline{(u'v')}^{++}}\right)}dy^+ \tag{7}$$

where Pr_t is the turbulent Pr. Similarly, for one heated wall, the temperature profile can be found from the following equation:

$$\overline{T}^+ = Pr\int_0^{y^+} \frac{(1+\gamma)\left(1-\frac{y^+}{2h^+}\right)}{1 + \frac{Pr}{Pr_t}\left(\frac{\overline{(u'v')}^{++}}{1-\overline{(u'v')}^{++}}\right)}dy^+ \tag{8}$$

where the correction term γ for two heated walls is calculated from the following equation:

$$\frac{q}{q_w} = (1+\gamma)\left(1 - \frac{y^+}{h^+}\right) = \frac{\left(1-\frac{y^+}{h^+}\right)\int_0^{y^+}\left[1-\overline{(u'v')}^{++}\right]\left(1-\frac{y^+}{h^+}\right)dy^+ + \int_{y^+}^{h^+}\left[1-\overline{(u'v')}^{++}\right]\left(1-\frac{y^+}{h^+}\right)^2 dy^+}{\int_0^{h^+}\left[1-\overline{(u'v')}^{++}\right]\left(1-\frac{y^+}{h^+}\right)^2 dy^+} \tag{9}$$

For one heated wall, the equivalent correlation is

$$\frac{q}{q_w} = (1+\gamma)\left(1 - \frac{y^+}{2h^+}\right) = \frac{\left(1-\frac{y^+}{2h^+}\right)\int_0^{y^+}\left[1-\overline{(u'v')}^{++}\right]\left(1-\frac{y^+}{2h^+}\right)dy^+ + \int_{y^+}^{h^+}\left[1-\overline{(u'v')}^{++}\right]\left(1-\frac{y^+}{2h^+}\right)^2 dy^+}{\int_0^{h^+}\left[1-\overline{(u'v')}^{++}\right]\left(1-\frac{y^+}{2h^+}\right)^2 dy^+} \tag{10}$$

To summarize, one needs empirical equations for $\overline{(u'v')}^{++}$ and Pr_t, in order to solve for the mean velocity and temperature according to this model.

2.3. Heat balance

The heat balance equations have been developed by Teitel and Antonia [8] for fully developed turbulent channel flow for different cases of heating as follows:

Case 1: Both walls are heated at the same constant heat flux uniformly and equally

$$\frac{1}{Pr}\frac{d\overline{T}^+}{dy^+} + \left(\overline{T'v'}^+\right) = \frac{q}{q_w} \tag{11}$$

Case 2: One wall (at $y^+ = 0$) is heated with constant heat flux uniformly and the second wall is kept adiabatic

$$\frac{1}{Pr}\frac{d\overline{T}^+}{dy^+} + (\overline{T'v'^+}) = \frac{q}{q_w} \tag{12}$$

Substituting Eq. (6) in (11) and (12) yields the following heat balances when the correction γ for the shear stress across the channel is taken into account:

$$\frac{1}{Pr}\frac{d\overline{T}^+}{dy^+} + (\overline{T'v'^+}) = \left(1 - \frac{y^+}{h^+}\right)(1+\gamma) \tag{13}$$

$$\frac{1}{Pr}\frac{d\overline{T}^+}{dy^+} + (\overline{T'v'^+}) = \left(1 - \frac{y^+}{2h^+}\right)(1+\gamma) \tag{14}$$

Eqs. (13) and (14) apply to Cases 1 and 2, respectively.

2.4. Direct numerical simulation

Details regarding the direct numerical simulation (DNS) algorithm used in the present work and its validation with experiments can be found in Lyons et al. [22] and in Gunther et al. [23]. The DNS of plane Couette flow has been discussed in [18,19]. The flow in both Poiseuille and Couette cases is for an incompressible, Newtonian fluid with constant properties. In Poiseuille channel flow, the flow is driven by the constant pressure gradient, and in plane Couette flow, the flow is driven by the constant shear stress caused by the two channel walls moving in opposite direction.

For Poiseuille flow, the Reynolds number, Re, was 2660 (based on the mean centerline velocity and the channel half-height). The simulation was done on a $128 \times 65 \times 128$ grid in the x, y, z directions, respectively. The dimensions of the computational box were $(4\pi h, 2h, 2\pi h)$ with $h = 150$ in wall units. The flow was periodic in the streamwise and spanwise directions. For the plane Couette flow, the Reynolds number was also 2660 (based on half the relative velocity of the two walls and the channel half-height). The simulation was done on $256 \times 65 \times 128$ grid with computational box dimensions $(8\pi h, 2h, 2\pi h)$. The computational box was doubled in the streamwise directions, relative to the plane channel flow, to take into account the large velocity structures reported in Couette flow [24–26].

2.5. Lagrangian scalar tracking method

The Lagrangian scalar tracking (LST) method was used to generate the mean temperature profiles, by tracking heat markers in the flow field created by the DNS. The motion of the heat markers was decomposed into a convection part and a molecular diffusion part. The convective part was calculated from the fluid velocity at the marker position. The velocity field resulting from the DNS was used to interpolate at each particle position with a sixth order Lagrange polynomial scheme in the streamwise and spanwise directions and a Chebyshev interpolation scheme in the wall normal direction [27]. The effect of molecular diffusion was simulated by imposing a 3-D random walk on the particle motion, which was added on the convective part of the motion after each time step, Δt, and took values from a Gaussian distribution with zero mean and standard deviation, $\sigma = \sqrt{2\Delta t/Pr}$, for each one of the three space dimensions in viscous wall units (this follows from the Brownian motion theory). The building block for the Lagrangian simulation was the probability function $P_1(X - x_0, Y, t - t_0|\vec{x}_0, t_0)$ that a heat marker released at the wall of the channel at $x = x_0$ at time t_0 is going to be at a location (X, Y) in the channel. The physical explanation for this probability function is that it represents temperature contours, or snapshots of a cloud of contaminants, released instantaneously at $x_0 = 0$. By integrating (or, in the discrete case, summing up) P_1 from time t_0 to a final time t_f, the behavior of a continuous line source, represented by the probability function P_2, can be obtained,

$$P_2(X - x_0, Y) = \sum_{t=t_0}^{t_f} P_1(X - x_0, Y, t|\vec{x}_0, t_0) \tag{15}$$

Details of all the Lagrangian runs used here were reported in [17] and [19]. In addition, raw data from the simulations are available on-line [28]. For Poiseuille channel flow, 16,129 markers were released instantaneously at the channel wall for high Pr, and 145,161 markers were released at a time for low Pr, (these are referred to as run E and run C, respectively, in Table 1 of Ref. [17]). For plane Couette flow, 145,161 markers were released instantaneously at the channel wall for all the Pr, referred as run A and run B in [19]. Descriptions and validations for the LST methodology can be found elsewhere [29–34].

The mean temperature profile can be synthesized using a series of continuous line sources covering one (the bottom), or two walls of the channel (both the top and the bottom). Heat flux added to the bottom wall can be simulated by integrating P_2 over the streamwise direction

$$\begin{aligned}\overline{T}(y) &\equiv \sum_{x=x_0}^{x_f} P_2(X - x_0, y|\vec{x}_0) \\ &= \sum_{x=x_0}^{x_f}\sum_{t=t_0}^{t_f} P_1(X - x_0, y, t - t_0|\vec{x}_0, t_0) \\ &t_f \to \infty \text{ and } x_f \to \infty\end{aligned} \tag{16}$$

The fully developed mean temperature for the case of heat flux from both planes, therefore, can be calculated using

$$\overline{T}(y) = \overline{T}(y) + \overline{T}(2h - y) \tag{17}$$

and assuming that the temperature is symmetric around the center-plane (i.e., the plane $y = h$). Details regarding the mean temperature profiles can be found in [17–19].

3. Results and discussion

3.1. Total shear stress due to turbulence

The fraction of the total shear stress due to turbulence, $\overline{(u'v')}^{++}$, based on the DNS results for channel and Couette flow, is presented in Fig. 1 as a function of the distance

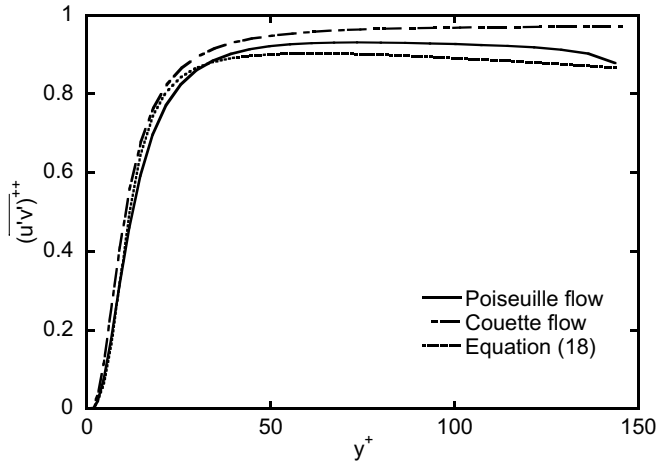

Fig. 1. Local fraction of shear stress due to turbulence in Poiseuille flow and Couette flow as a function of normal distance from the wall, compared with Churchill's correlation (Eq. (18)). The simulations are for $h^+ = 150$.

from the channel wall. This fraction goes from zero at the channel wall to almost one at the center of the channel. As shown in Fig. 1, the fraction of total shear stress due to turbulence in channel flow is smaller than that of Couette flow at the same distance from the wall.

A correlation equation for the turbulent shear stress $\overline{(u'v')}^{++}$ has been introduced by Danov et al. [21] in the form of a power mean of three limiting expressions for $\overline{(u'v')}^{++}$ (the asymptotes for $y^+ \to 0$ and $y^+ \to h^+$, and an exponential decay for the logarithmic region $30 < y^+ < 0.1h^+$). The turbulent shear stress is calculated based on the half channel height and the distance from the wall as in the following equation:

$$\overline{(u'v')}^{++} = \left(\left[0.7 \left(\frac{y^+}{10} \right)^3 \right]^{-8/7} + \left| \exp\left\{ \frac{-1}{0.436 y^+} \right\} - \frac{1}{0.436 h^+} \left(1 + \frac{6.95 y^+}{h^+} \right) \right|^{-8/7} \right)^{-7/8} \quad (18)$$

A plot of this correlation varying with the distance from the wall is also presented in Fig. 1. It is close to the profile for Poiseuille flow but it is smaller than the Couette flow profile. It should be noted that the coefficients 0.436 and 6.95 in Eq. (18) were obtained based on measurements for pipe flow in the Princeton superpipe [35] for very high Reynolds numbers. These data have now been updated [36], but predictions of $\overline{(u'v')}^{++}$ and of temperature profiles based on updated coefficients have not been found to differ significantly than using Eq. (18) [16].

3.2. Normal heat flux

The normal heat flux is found using Eqs. (13) and (14) for one heated wall and two heated walls, respectively. The heat flux as a function of y for one heated wall is presented in Fig. 2(a) and (b). As the Pr increases, the normal heat flux increases. As seen in Fig. 2(a) and (b), the normal heat flux increases to a maximum of 1 for high Pr, and less than 1 for low Pr. For high Pr, such as 2400 and up, this maximum occurs very close to the wall. The normal heat flux is approximately 0.55 at half channel height for all the Prandtl numbers.

The normal heat flux in the case where both walls are heated uniformly and equally is shown in Fig. 3(a) and (b) for Poiseuille flow and Couette flow, respectively. It follows the same trends as in the one heated wall case: the normal heat flux increases as Pr increases. The normal heat flux reaches a maximum pretty fast, and then decreases to zero at half channel height. The result for $Pr = 0.7$ shows a very good agreement with previously reported normal heat flux by Kasagi et al. [37]. Results from Kawamura et al. [9] and Kim and Moin [38] for $Pr = 0.7$ are also shown in Fig. 3(a).

The fraction of the normal heat flux due to turbulence is presented in Fig. 4(a) and (b) for one heated wall and Fig. 5(a) and (b) for two heated walls. In Fig. 4(a), for Poiseuille channel flow with one heated wall, this fraction

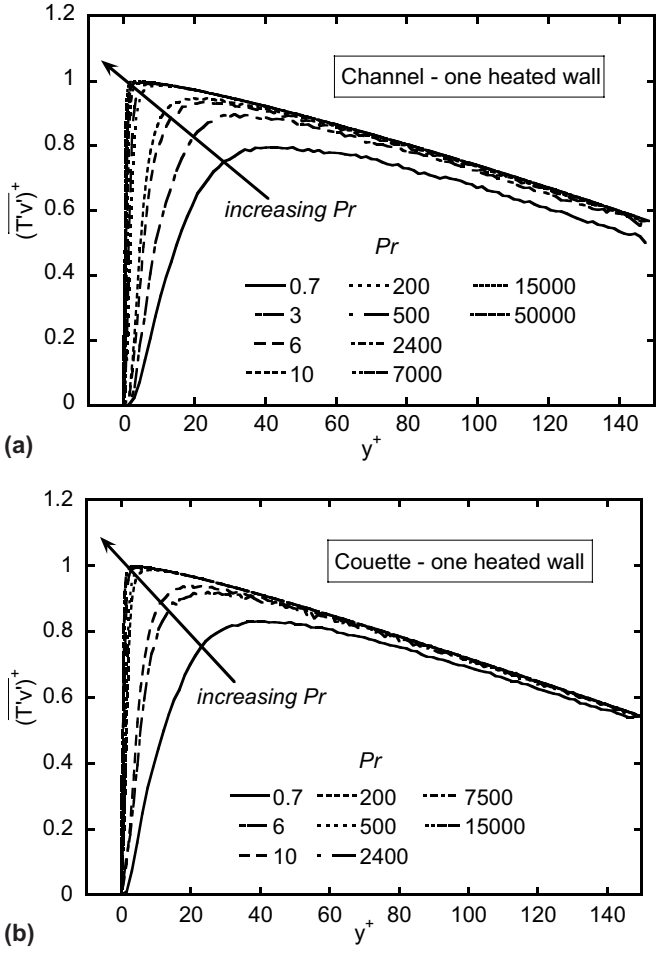

Fig. 2. Normal heat fluxes as function of normal position for the case of uniform heating from one plate for (a) Poiseuille channel, and (b) Couette flow. The simulations are for $h^+ = 150$.

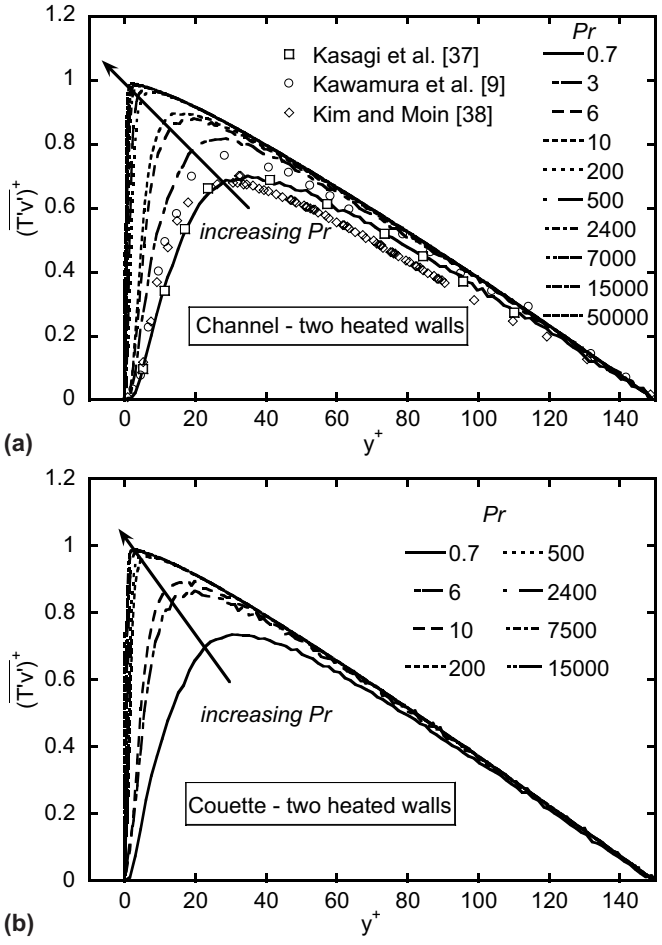

Fig. 3. Normal heat fluxes as function of normal position for the case of uniform and equal heating from two plates for (a) Poiseuille channel (data points from Kasagi et al. [37], Kawamura et al. [9] and Kim and Moin [38]), and (b) Couette flow. The Lagrangian simulations are for $h^+ = 150$.

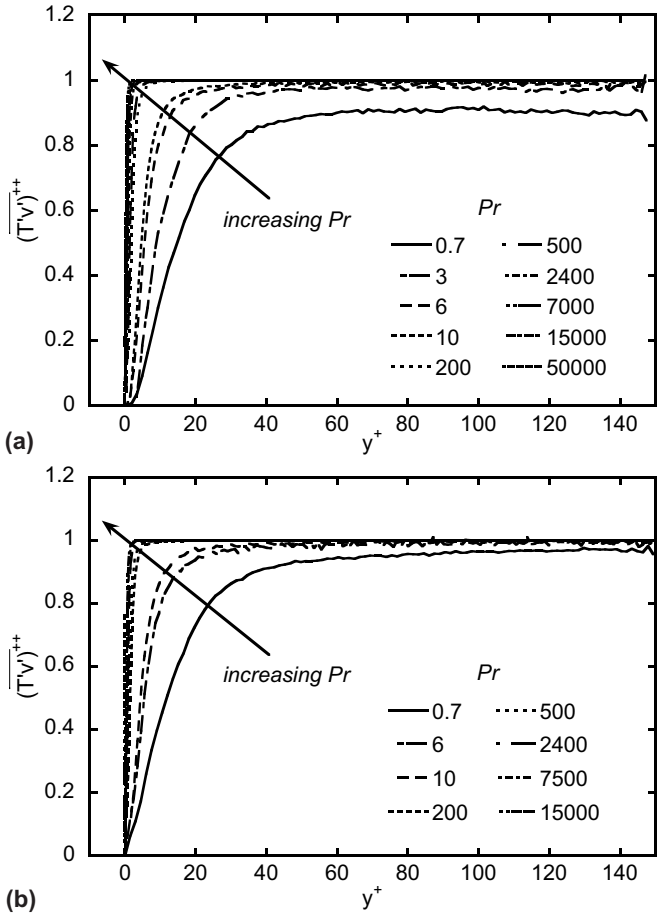

Fig. 4. Turbulent heat flux as function of normal position for the case of uniform heating from one plate for (a) Poiseuille channel and (b) Couette flow ($h^+ = 150$ for both cases).

increases to 1 quickly (e.g., $y^+ \approx 40$ for $Pr = 6$, 10; $y^+ \approx 10$ for $Pr = 200$, 5000 and $y^+ \approx 2$ for $Pr \geqslant 2400$) and then stays constant. This means that the normal heat flux is only due to turbulence. The normal heat flux for Couette flow with one heated wall is shown in Fig. 4(b) to exhibit the same trend. However, it increases to 1 faster than in Poiseuille channel flow. For low Pr in both cases, the fraction never gets to 1, even at the center of the channel. The heat flux is affected by both convection and diffusion throughout the channel for low Pr.

The normal heat flux for the case where both walls are heated uniformly and equally is shown in Fig. 5(a) and (b). The results look similar to the results in Fig. 4(a) and (b). It does not matter if one wall or two walls are heated; it takes the same distance to get to the turbulence effects-only region for all the Pr.

3.3. Mean temperature

The temperature profiles for the case when one wall is heated constantly are shown in Fig. 6(a) and (b) for Poiseuille channel flow and Couette flow, respectively, and in Fig. 7(a) and (b) for the two heated walls case. The temperatures presented in the figures were calculated using the following methods:

Method 1: Using DNS/LST method – the mean temperature profiles have been presented previously in Refs. [17,19].

Method 2: Using Churchill's prediction (Eqs. (7) and (8)), where the turbulent Prandtl number, Pr_t, is calculated from our DNS/LST data as follows:

$$Pr_t = \frac{E_v}{E_\alpha} \quad \text{and} \quad E_\alpha = \frac{\overline{(T'v')^+}}{\frac{d\overline{T}^+}{dy^+}} \quad \text{and} \quad E_v = \frac{\overline{(u'v')^+}}{\frac{d\overline{U}^+}{dy^+}} \tag{19}$$

and $\overline{(u'v')^{++}}$ is also from DNS/LST data as presented in Fig. 1.

Method 3: Using Churchill's correlation for $\overline{(u'v')^{++}}$ as in Eq. (18), and direct calculation of turbulent Prandtl number Pr_t from our DNS/LST data.

Method 4: Using the Kays empirical correlation for Pr_t [39] and the DNS/LST-obtained $\overline{(u'v')^{++}}$. The correlation suggested by Kays, $Pr_t = \frac{0.7\nu}{Pr\nu_t} + 0.85$ (where ν_t is the eddy viscosity), has been written in terms of $\overline{(u'v')^{++}}$ (using Eq.

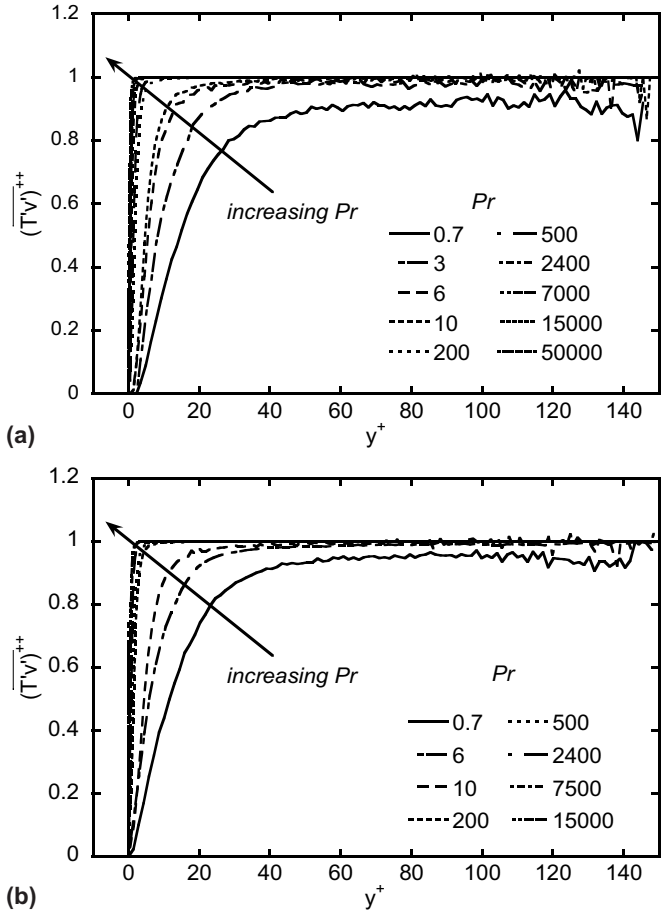

Fig. 5. Turbulent heat flux as function of normal position for the case of uniform and equal heating from two plates for (a) Poiseuille channel and (b) Couette flow ($h^+ = 150$ for both cases).

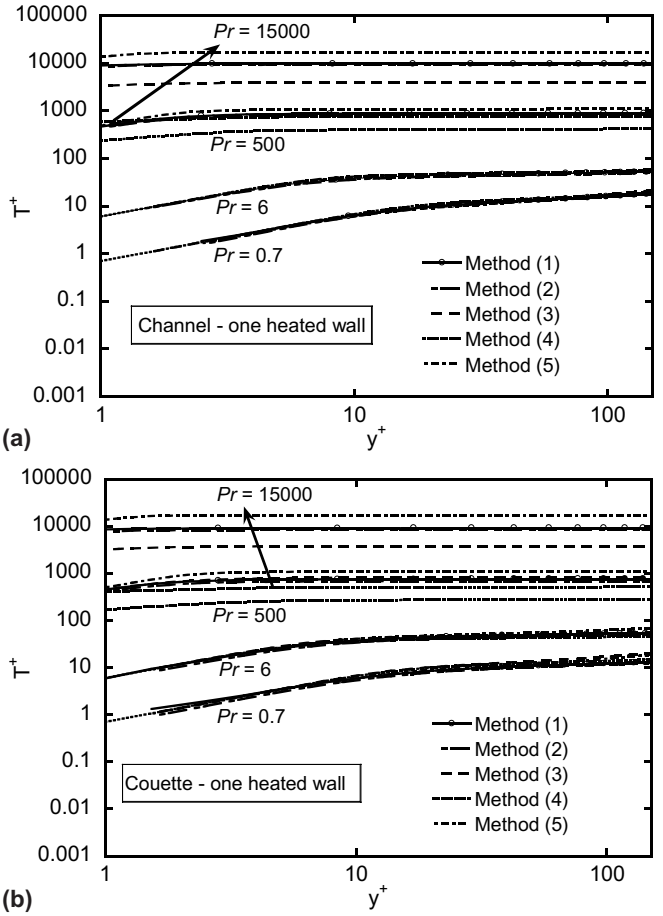

Fig. 6. Temperature predictions using different methods compared to DNS/LST data for the case of uniform heating from one plate for (a) Poiseuille channel and (b) Couette flow ($h^+ = 150$ for both cases).

(4) and the definition of $\overline{(u'v')^{++}}$ one can see that $[1-\overline{(u'v')^{++}}]/\overline{(u'v')^{++}} = \nu/\nu_t$) in the following form [12]:

$$Pr_t = \frac{0.7[1-\overline{(u'v')^{++}}]}{Pr\overline{(u'v')^{++}}} + 0.85 \tag{20}$$

Since Kays suggested that the coefficient 2.0 works better than 0.7 for low Pr fluids, we used 2.0 for $Pr < 1$.

Method 5: Using Eq. (18) for $\overline{(u'v')^{++}}$ and Eq. (20) for Pr_t.

For low and medium Pr, the temperature profiles were predicted within reasonable errors (hardly seen in the logarithmic scale in Figs. 6 and 7). However, for high Pr ($Pr = 500$ and 15,000 in the plots, and other Pr from 100 and up), Churchill's prediction gives a good agreement with the DNS/LST results. However, if $\overline{(u'v')^{++}}$ from Eq. (18) or Kays empirical solution for Pr_t from Eq. (20) is used, the variations are high. These variations are shown in Table 1 (for one heated wall) and in Table 2 (for two heated walls) for Poiseuille flow and Couette flow, respectively. When using Method 1, the results are consistent and within 10% error. When using other methods, the errors are high for very high Pr or very low Pr. These methods give reasonable results for low to medium Pr (from 0.1 to 10). The sensitivity of these variations to the change of $\overline{(u'v')^{++}}$ is high, considering that $\overline{(u'v')^{++}}$ is only slightly different from the value obtained from DNS.

The results appearing in Tables 1 and 2 should not be very surprising. They clearly validate the algebraic model predictions when $\overline{(u'v')^{++}}$ and Pr_t are calculated directly using our data, instead of employing empiricisms applicable to other, different situations. In fact, Churchill's derivations have been developed for high Re cases ($h^+ > 300$) and for Pr applicable to heat transfer ($Pr \leqslant 100$). Eq. (18) in particular, is expected to work better for $h^+ > 300$ – the lower limit for the development of a logarithmic region in the mean velocity profile, which is necessary for the derivation of Eq. (18). It should also be noted that Pr on the order of thousands applies to cases of mass transfer rather than heat transfer, so one should more accurately think of these cases as high Schmidt number cases. Even though it would be very convenient to use Eqs. (18) and (20) to estimate the temperature in a turbulent flow field, the results for this method of calculation are acceptable only for specific cases of Pr. Calculations that are based on publicly

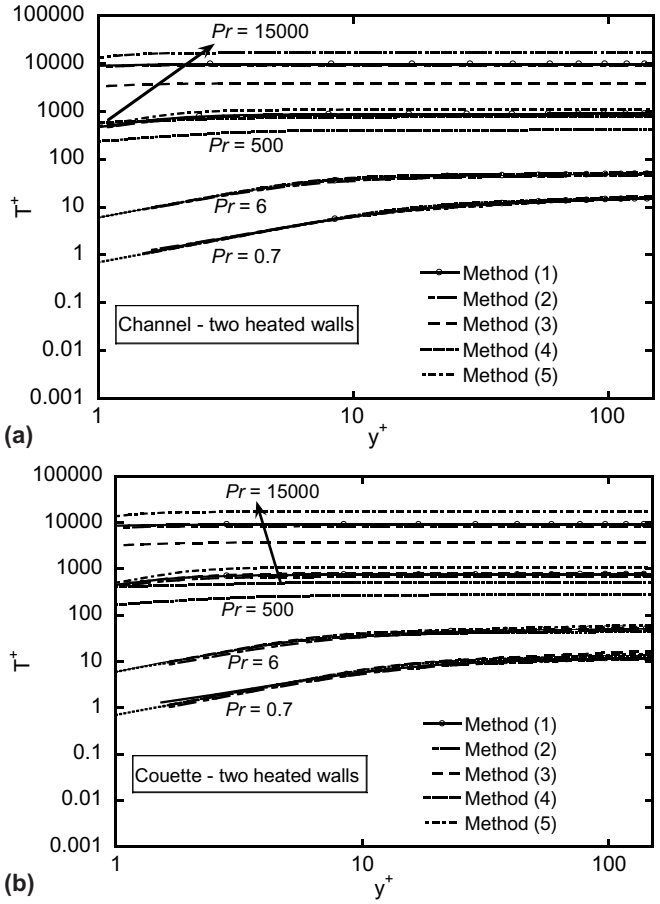

Fig. 7. Temperature predictions using different methods compared to DNS/LST data for the case of uniform and equal heating from two plates for (a) Poiseuille channel and (b) Couette flow ($h^+ = 150$ for both cases).

available data from Eulerian DNS [40] also support the above conclusions (the data are from the University of Tokyo web site, for fully developed thermal field in 2D turbulent channel flow, with $Pr = 0.71$, $h^+ = 150$, $Re = 2280$, generated by the code CH122_PG.WL1). Analysis of these data in a similar manner as in Table 2 (i.e., using the Eulerian DNS data instead of the LST/DNS data, and comparing the results of each method to the Eulerian DNS results) shows an error of 2.847% when using Method 2; 4.579% for Method 3; 8.003% for Method 4; and 8.389% for Method 5.

Since the model predictions appear to deviate from the simulation results mostly at high Pr, one could attempt to find a correction for this case. Sensitivity analysis of the prediction model [16] demonstrated that the predictions are not very sensitive on the values of the constants appearing in Eq. (18). It could be then practical to introduce a correction factor, C_f, in Eqs. (7) and (8) as follows:

$$\overline{T}^+ = Pr \int_0^{y^+} \frac{(1+\gamma)\left(1-\frac{y^+}{h^+}\right)}{1 + C_f * \frac{Pr}{Pr_t}\left(\frac{\overline{(u'v')^{++}}}{1-\overline{(u'v')^{++}}}\right)} \mathrm{d}y^+$$

for two heated walls (21)

Table 1
Errors of predicted temperatures for one heated wall using different methods; Percent error $= \frac{|T-T_{\text{Method 1}}|}{T_{\text{Method 1}}} * 100\%$: (a) Poiseuille channel flow ($h^+ = 150$), and (b) Couette flow ($h^+ = 150$)

Pr	Method (2)	Method (3)	Method (4)	Method (5)
Panel a: Poiseuille flow, error (%)				
0.010	10.241	205.094	16.224	16.076
0.025	4.234	5.762	13.422	12.689
0.050	7.959	5.042	14.795	12.964
0.1	0.587	3.883	1.274	4.033
0.7	2.601	4.959	7.708	9.494
1	5.865	4.005	21.892	23.107
3	0.789	3.264	4.634	4.368
6	4.558	1.924	6.294	7.910
10	5.945	1.530	3.119	6.282
200	8.913	14.924	33.134	6.512
500	7.428	24.218	52.402	5.371
2400	5.222	50.012	75.318	17.432
7000	4.066	69.184	85.576	49.639
15,000	4.295	70.666	91.548	60.165
50,000	5.750	98.809	95.843	77.605
Panel b: Couette flow, error (%)				
0.1	8.327	15.277	8.295	27.231
0.7	5.795	19.420	13.910	33.440
6	7.747	16.758	12.066	3.022
10	9.141	14.852	12.456	4.556
200	14.543	37.544	43.112	20.002
500	11.467	44.229	62.813	7.808
2400	9.029	61.573	83.107	16.063
7500	8.629	80.087	90.685	40.994
15,000	8.751	87.041	93.785	58.640

Table 2
Errors of predicted temperatures for two heated walls using different methods, Percent error $= \frac{|T-T_{\text{Method 1}}|}{T_{\text{Method 1}}} * 100\%$: (a) Poiseuille channel flow ($h^+ = 150$), and (b) Couette flow ($h^+ = 150$)

Pr	Method (2)	Method (3)	Method (4)	Method (5)
Panel a: Poiseuille flow, error (%)				
0.010	29.277	100.663	22.630	22.514
0.025	5.596	15.553	14.352	13.727
0.050	4.498	5.780	12.781	11.243
0.1	1.441	2.212	1.163	3.837
0.7	0.549	2.890	9.509	9.898
3	1.411	3.026	3.367	2.821
6	4.899	1.714	7.676	8.784
10	6.214	2.276	2.156	4.892
200	8.907	16.707	33.209	1.233
500	7.443	24.226	52.458	5.419
2400	5.227	50.036	75.343	17.449
7000	4.150	71.813	85.590	39.051
15,000	4.294	70.671	91.556	60.173
50,000	5.751	98.813	95.847	77.612
Panel b: Couette flow, error (%)				
0.1	9.881	32.989	5.841	20.486
0.7	6.053	12.896	13.995	29.063
6	8.256	14.433	11.099	2.930
10	9.494	13.066	11.691	4.540
200	14.546	37.582	43.033	20.163
500	11.491	44.185	62.801	7.893
2400	9.042	61.590	83.117	16.052
7500	8.640	80.067	90.689	40.977
15,000	8.754	87.109	93.782	58.596

Table 3
Correction factor and percent errors of predicted temperatures when applying a correction factor for Method (3); Percent error $= \frac{|T-T_{\text{Method 1}}|}{T_{\text{Method 1}}} * 100\%$: (a) Poiseuille channel flow ($h^+ = 150$), and (b) Couette flow ($h^+ = 150$)

Pr	One heated wall		Two heated walls	
	C_f	Error (%)	C_f	Error (%)
Panel a				
0.01	1.0	23.098	0.9	12.798
0.025	1.2	4.121	0.9	9.004
0.05	1.1	3.602	0.9	2.180
0.1	1.3	2.009	1.1	1.604
0.7	1.0	4.959	1.0	2.890
3	1.0	3.264	0.9	2.810
6	1.0	1.924	1.0	1.715
10	1.0	1.530	0.9	1.315
200	1.7	0.710	1.9	1.203
500	2.8	0.852	2.8	0.881
2400	7.2	0.753	7.2	0.748
7000	6.8	0.519	10.0	0.480
15,000	8.2	0.250	8.2	0.245
50,000	6.0	0.268	6.0	0.267
Panel b				
0.1	1.8	8.998	1.2	5.516
0.7	1.5	7.417	1.4	4.576
6	1.5	3.505	1.4	2.338
10	2.4	2.531	1.4	1.587
200	4.2	1.075	4.2	0.996
500	6.0	0.795	6.0	0.769
2400	11.0	0.579	10.9	0.430
7500	12.3	0.266	12.3	0.232
15,000	10.4	0.208	10.4	0.200

and

$$\overline{T}^+ = Pr \int_0^{y^+} \frac{(1+\gamma)\left(1-\frac{y^+}{2h^+}\right)\mathrm{d}y^+}{1 + C_f * \frac{Pr}{Pr_t}\left(\frac{\overline{(u'v')^{++}}}{1-\overline{(u'v')^{++}}}\right)}\mathrm{d}y^+$$

for one heated wall (22)

The practical advantage of using this correction factor is that now we need to search for the values of one parameter, instead of the values for four parameters that appear in Eq. (18). However, by introducing C_f we introduce empiricism in Eqs. (7) and (8), reducing, thus, their purity. This coefficient C_f is only dependent on Pr. Given this reservation, Table 3 shows the values of C_f that can be used with Method 3 and the errors associated with these values. It can be seen that a choice of C_f at around 10 can reduce the errors to less than 1% for the large values of Pr ($Pr \geqslant 500$).

4. Conclusions

An investigation of the recent theory for turbulent convection developed by Churchill and coauthors has been presented. According to the Churchill model, fully developed flow and convection can be expressed as local fractions of the shear stress and the heat flux density due to turbulent fluctuations; and the fully developed temperature can be predicted if the velocity field and the turbulent Prandtl number are known. In effect, the model suggests that the mean temperature scales with the fraction of the heat flux due to turbulence. Application of the theory for an extensive range of fluids and for different turbulence structures and comparison to Lagrangian simulation results shows a deviation of less than 10% for most Pr, even though the model equations were developed for flows with higher Reynolds numbers than those employed by DNS. The main contributions to these deviations were due to the use of a model for Pr_t and for $\overline{(u'v')}^{++}$. A correction factor can be introduced for very high Pr fluids, which can provide model predictions that are within 1% of the simulation results.

Acknowledgements

The support of NSF under CTS-0209758 is gratefully acknowledged. This work was also supported by the National Computational Science Alliance under CTS-040023 and utilized the NCSA IBMp690 and the NCSA SGI/CRAY Origin2000. Computational support was also offered by the University of Oklahoma Center for Supercomputing Education and Research (OSCER).

References

[1] D.S. Finnicum, T.J. Hanratty, Effects of favorable pressure gradients on turbulent boundary layers, AIChE J. 34 (1) (1988) 529–540.
[2] T. Wei, W.W. Willmarth, Reynolds number effects on the structure of a turbulent channel flow, J. Fluid Mech. 204 (1989) 57–95.
[3] K.R. Sreenivasan, The turbulent boundary layer, in: M. Gad-el-Hak (Ed.), Frontiers in Experimental Fluid Mechanics, Lecture Notes in Engineering, vol. 46, Springer-Verlag, Berlin, 1989, pp. 159–209.
[4] T.J. Hanratty, D.V. Papavassiliou, The role of wall vortices in producing turbulence, in: R.L. Panton (Ed.), Self Sustaining Mechanisms of Wall Turbulence, Computational Mechanics Inc., 1997, pp. 83–108.
[5] G.I. Barenblatt, A.J. Chorin, V.M. Prostokishin, A note on the intermediate region in turbulent boundary layers, Phys. Fluids 12 (9) (2000) 2159–2161.
[6] G.I. Barenblatt, A.J. Chorin, V.M. Prostokishin, Self-similar intermediate structures in turbulent boundary layers at large Reynolds numbers, J. Fluid Mech. 410 (2000) 263–283.
[7] T. Wei, P. Fife, J. Klewicki, P. McMurtry, Properties of the mean momentum balance in turbulent boundary layer, pipe and channel flows, J. Fluid Mech. 522 (2005) 303–327.
[8] M. Teitel, R.A. Antonia, Heat transfer in fully developed turbulent channel flow: comparison between experiment and direct numerical simulations, Int. J. Heat Mass Transfer 36 (6) (1993) 1701–1706.
[9] H. Kawamura, K. Ohsaka, H. Abe, K. Yamamoto, DNS of turbulent heat transfer in channel flow with low to medium–high Prandtl number fluid, Int. J. Heat Fluid Flow 19 (1998) 482–491.
[10] H. Kawamura, H. Abe, Y. Matsuo, DNS of turbulent heat transfer in channel flow with respect to Reynolds and Prandtl number effects, Int. J. Heat Fluid Flow 20 (1999) 196–207.
[11] S.W. Churchill, C. Chan, Turbulent flow in channels in terms of the turbulent shear and normal stresses, AIChE J. 41 (1995) 2513–2521.
[12] S.W. Churchill, Progress in the thermal sciences: AICHE Institute Lecture, AIChE J. 46 (9) (2000) 1704–1722.
[13] B. Yu, H. Ozoe, S.W. Churchill, The characteristics of fully developed turbulent convection in a round tube, Chem. Eng. Sci. 56 (2001) 1781–1800.

[14] S.W. Churchill, A reinterpretation of the turbulent Prandtl number, Ind. Eng. Chem. Res. 41 (2002) 6393–6401.
[15] B.A. Kader, Temperature and concentration profiles in fully turbulent boundary layers, Int. J. Heat Mass Transfer 29 (9) (1981) 1541–1544.
[16] S.W. Churchill, B. Yu, Y. Kawaguchi, The accuracy and parametric sensitivity of algebraic models for turbulent flow and convection, Int. J. Heat Mass Transfer 48 (24–25) (2005) 5488–5503.
[17] B.M. Mitrovic, P.M. Le, D.V. Papavassiliou, On the Prandtl or Schmidt number dependence of the turbulence heat or mass transfer coefficient, Chem. Eng. Sci. 59 (3) (2004) 543–555.
[18] P.M. Le, D.V. Papavassiliou, Turbulent dispersion from elevated sources in channel and Couette flow, AIChE J. 51 (9) (2005) 2402–2414.
[19] P.M. Le, D.V. Papavassiliou, Turbulent heat transfer in plane Couette flow, J. Heat Transfer – Trans. ASME 128 (2006) 53–62.
[20] L. Heng, C. Chan, S.W. Churchill, Essentially exact characteristics of turbulent convection in a round tube, Chem. Eng. J. 71 (1998) 163–173.
[21] S.N. Danov, N. Arai, S.W. Churchill, Exact formulations and nearly exact numerical solutions for convection in turbulent flow between parallel plates, Int. J. Heat Mass Transfer 43 (2000) 2767–2777.
[22] S.L. Lyons, T.J. Hanratty, J.B. McLaughlin, Large-scale computer-simulation of fully-developed turbulent channel flow with heat-transfer, Int. J. Numer. Meth. Fluids 13 (8) (1991) 999–1028.
[23] A.D. Gunther, D.V. Papavassiliou, M.D. Warholic, T.J. Hanratty, Turbulent flow in channel at low Reynolds number, Exp. Fluids 25 (1998) 503–511.
[24] D.V. Papavassiliou, T.J. Hanratty, Interpretation of large scale structures observed in a turbulent plane Couette flow, Int. J. Heat Fluid Flow 18 (1997) 55–69.
[25] J. Komminaho, A. Lundbladh, A.V. Johansson, Very large structures in plane turbulent Couette flow, J. Fluid Mech. 320 (1996) 259–285.
[26] K.H. Bech, N. Tillmark, P.H. Alfredson, H.I. Anderson, An investigation of turbulent plane Couette flow at low Reynolds numbers, J. Fluid Mech. 286 (1995) 291–325.
[27] K. Kontomaris, T.J. Hanratty, J.B. McLaughlin, An algorithm for tracking fluid particles in a spectral simulation of turbulent channel flow, J. Comput. Phys. 103 (1993) 231–242.
[28] D.V. Papavassiliou group, Computational Transport Processes, University of Oklahoma, World Wide Web pages. Available from: <http://129.15.119.70/home.html> (accessed 09.08.05).
[29] D.V. Papavassiliou, T.J. Hanratty, The use of Lagrangian methods to describe turbulent transport of heat from the wall, Ind. Eng. Chem. Res. 34 (1995) 3359–3367.
[30] D.V. Papavassiliou, T.J. Hanratty, Transport of a passive scalar in a turbulent channel flow, Int. J. Heat Mass Transfer 40 (1997) 1303–1311.
[31] S.S. Ponoth, J.B. McLaughlin, Numerical simulation of a mass transfer for bubbles in water, Chem. Eng. Sci. 55 (2000) 1237–1255.
[32] D.V. Papavassiliou, Scalar dispersion from an instantaneous line source at the wall of a turbulent channel for medium and high Prandtl number fluids, Int. J. Heat Fluid Flow 23 (2002) 161–172.
[33] D.V. Papavassiliou, Turbulent transport from continuous sources at the wall of a channel, Int. J. Heat Mass Transfer 45 (2002) 3571–3583.
[34] Y. Mito, T.J. Hanratty, Lagrangian stochastic simulation of turbulent dispersion of heat markers in a channel flow, Int. J. Heat Mass Transfer 46 (6) (2003) 1063–1073.
[35] M.V. Zagarola, Mean-flow scaling of turbulent pipe flow, PhD Thesis, Princeton University, Princeton, NJ, 1996.
[36] B.J. McKeon, J. Li, W. Jiang, J.F. Morisson, A.J. Smits, Further observations on the mean velocity in fully-developed pipe flow, J. Fluid Mech. 501 (2004) 135–147.
[37] N. Kasagi, Y. Tomita, A. Kuroda, Direct numerical simulation of a passive scalar field in a turbulent channel flow, J. Heat Transfer – Trans. ASME 114 (1992) 598–606.
[38] J. Kim, P. Moin, in: J.C. Andre, J. Cousteix, F. Durst, B.E. Launder, F.W. Schmidt, J.H. Whitelaw (Eds.), Transport of passive scalars in a turbulent channel flow, Turbulent Shear Flows, vol. 6, Springer, Berlin, 1989, p. 85.
[39] W.M. Kays, Turbulent prandtl number – where are we? J. Heat Transfer – Trans. ASME 116 (1994) 284–295.
[40] N. Kasagi, Turbulent heat transfer, University of Tokyo, World Wide Web page. Available from: <http://www.thtlab.t.u-tokyo.ac.jp/> (accessed 09.08.05).